Functionally non-redundant paralogs *spe-47* and *spe-50* encode FB-MO associated proteins and interact with *him-8*

Jessica N. Clark, Gaurav Prajapati, Fermina Aldaco, Thomas J. Sokolich, Steven Keung, Sarojani Austin, Ángel A. Valdés, and Craig W. LaMunyon*

Department of Biological Sciences, Cal Poly Pomona, Pomona, California, United States of America

*Corresponding author

email: cwlamunyon@cpp.edu

Abstract

The activation of *C. elegans* spermatids to crawling spermatozoa is affected by a number of genes including *spe-47*. Here, we investigate a paralog to *spe-47*: *spe-50,* which has a highly conserved sequence and expression, but which is not functionally redundant to *spe-47*. Phylogenetic analysis indicates that the duplication event that produced the paralogs occurred prior to the radiation of the *Caenorhabditis* species included in the analysis, allowing a long period for the paralogs to diverge in function. Furthermore, we observed that knockout mutations in both genes, either alone or together, have little effect on sperm function. However, hermaphrodites harboring both knockout mutations combined with a third mutation in the *him-8* gene are nearly self-sterile due to a sperm defect, even though they have numerous apparently normal sperm within their spermathecae. We suggest that the sperm in these triple mutants are defective in fusing with oocytes, and that the effect of the *him-8* mutation is due to its role in chromatin remodeling.

Introduction

Sperm cells generally face a brief life of intense competition to realize their goal of fertilizing an oocyte. To have success, they must execute with extreme efficiency. They must activate at precisely the right moment, locomote with haste using chemotaxis to guide them to the fertilization site, and fuse with an oocyte as quickly as possible. All this is required of a cell stripped of its ability to express its genome, in most cases surviving only on the meager stores within its tiny volume. Given the unusual nature of sperm cells, it is not surprising that well in excess of 1,000 genes are specific to, or upregulated in, sperm development [1, 2].

Our studies are concerned with the activation of sperm from the nematode *C. elegans.* Spherical and immotile, *C. elegans* spermatids are so primed to activate that they require the activity of SPE-6 to remain in the spermatid stage [3]. Once a signal is received, the spermatids undergo rapid wholesale cellular reorganization that involves an influx of cations [4], a brief elevation in pH [5], the release of intracellular Ca^{2+} [6-8], induction of a MAPK cascade [9], and polymerization of major sperm protein (MSP) and fusion of the membranous organelles (MOs) with the plasma membrane [7]. As a result, a pseudopod is extended and motility is achieved through MSP mediated pseudopodal treadmilling [10].

As the first step in the life of a *C. elegans* sperm cell, activation (spermiogenesis) may be initiated via two redundant pathways. One pathway, utilized only in males, involves the extracellular signaling serine protease TRY-5, which is secreted with the seminal fluid [11] and activates the spermatid. TRY-5 interacts with the transporter protein SNF-10 to stimulate activation [12]. The second pathway present in both males and hermaphrodites proceeds through the SPE-8 group proteins, namely, SPE-8, SPE-12, SPE-19, SPE-27, SPE-29 [reviewed in 13], and the most recent addition, SPE-43 [14]. It is thought that these proteins are anchored to the plasma membrane and transduce the activation signal inward, perhaps through the non-receptor tyrosine kinase SPE-8, which appears to move inward, away from the plasma membrane, during activation [15].

Our focus has been on discovering the identities of a collection of mutations recovered from a suppressor screen of *spe-27(it132ts)* [3]. Mutant *spe-27* hermaphrodites are sterile because their self-sperm do not activate. The suppressor mutations restore varying degrees of fertility due to the fact that they cause sperm to activate prematurely without the need for activation signal transduction. We have identified *spe-27(it132ts)*

63 suppressor mutations in *spe-4(hc196)* [16], *spe-46(hc197)* [17], and *spe-47(hc198)* [18].
64 There is a paralog to *spe-47* in the *C. elegans* genome with the sequence identifier
65 Y48B6A.5. Here, we report that this paralog is a new sperm gene designated *spe-50,* but it
66 is not functionally redundant to *spe-47*. However, knockouts of the two genes have an
67 unusual genetic interaction with *him-8* when combined in a triple mutant strain.

68 ## Methods

69 ### Worm strains and handling

70 All *C. elegans* strains were maintained on *Escherichia coli* OP50-seeded Nematode
71 Growth Media (NGM) agar plates [19]. The *Caenorhabditis* Genetic Center kindly provided
72 the following strains: N2, BA963: *spe-27(it132ts) IV,* BA966: *spe-27(it132ts) unc-22(e66) IV,*
73 CB1489: *him-8(e1489) IV,* DR466: *him-5(e1490) V,* BA17: *fem-1(hc17ts) IV,* JK654: *fem-*
74 *3(q23ts) IV,* EG5767: *qqIr7 I; oxSi78 II ; unc-119(ed3) III*, and SP444 *unc-4(e120) spe-*
75 *7(mn252)/mnC1* [*dpy-10(e128) unc-52(e444)*] *II*. Strain IE4488 harboring the *ttTi4488*
76 Mos1 transposon insertion in Y48B6A.5 was received from the NEMAGENETAG consortium
77 [20], and the transposon insertion was homozygosed to create strain ZQ117. Steven
78 L'Hernault kindly provided BA771 *spe-18(hc133)/mnC1* [*dpy-10(e128) unc-52(e444)*] *II.*
79 Other strains were created by combining alleles. Brood size was measured by counting the
80 progeny laid daily by hermaphrodites isolated in 35 mm petri dishes. In some cases, the
81 effect of mating on hermaphrodite fertility was assessed, in which case individual
82 hermaphrodites were maintained with four males each.

RT-PCR

To perform RT-PCR, RNA was extracted from mixed-age populations of worms. Large populations of each strain were collected and rinsed 4 times with M9 buffer. After freezing at -80 °C, the worms were disrupted by sonication in TRI reagent, and the RNA was extracted using the Direct-zol™ RNA purification kit following the manufacturer's protocol for DNase I digestion (Zymo Research). cDNA was synthesized with Maxima Reverse Transcriptase (Thermo Scientific™) and oligo(dT)18 primer (#SO131 Thermo Scientific™). cDNAs were adjusted to give the same concentration across samples prior to PCR amplification. A 536 bp region of *spe-50* cDNA was amplified from exons 3 and 4 with primers that flank the *ttTi4488* Mos1 insertion site (Forward primer: 5'-TTGACTTCTGTGCCTCCAGC -3'; Reverse primer: 5'-GGTTCAACAGATTCTTCCTCAAGTGG-3'). To determine if gene expression was upregulated in sperm, we multiplexed *spe-50* specific primers with primers that amplify an 898 bp region of the transcript of *act-2,* the *C. elegans* ortholog of β-Actin (Forward primer: 5'-GTATGGGACAGAAAGACTCG-3'; Reverse primer: 5'-ATAGATCCTCCGATCCAGAC-3'). The primers spanned intronic regions to distinguish between products from genomic DNA and cDNA. To determine if the *ttTi4488* Mos1 transposon insertion disrupted *spe-50* transcription, we compared RT-PCR from a population of *spe-50(ttTi4488)* with that from an N2 population. To determine if the *spe-50* transcript is upregulated in sperm, we compared RT-PCR products from populations of *fem-3(q23ts)*, hermaphrodites of which make only sperm, with products from *fem-1(hc13ts),* hermaphrodites of which make only oocytes.

CRISPR/Cas9-induced mutations

To induce specific mutations, we utilized the co-conversion strategy for CRISPR/Cas9 mediated gene edits [21]. Briefly, this strategy induces the dominant *cn64* mutation in the *dpy-10* gene in addition to the desired gene-specific edit. F1 worms heterozygous for *cn64* roll while they crawl and are more likely to also harbor the desired edit than do non-rollers [21]. Our two specific edits were accomplished by different methods. To create a mutation that replicates the *spe-47(hc198)* amino acid substitution in *spe-50,* we utilized the expression vector pDD162, which has both a single guide RNA (sgRNA) backbone and the Cas9 gene for *C. elegans* expression [22] (obtained from Addgene). The *spe-50* target sequence (5'-GATCTTGTTACAGTTCCAT-3') was chosen using a CRISPR guide-finding feature in Geneious R11 (https://www.geneious.com) based upon a high predicted on-target activity [23] and a low likelihood of off-target activity. The targeting sequence was inserted into the sgRNA cassette of pDD162 using the Q5® Site-Directed Mutagenesis Kit (New England BioLabs, Inc.), resulting in identical plasmids (pTS11 and pTS12).

To make the specific *spe-50* edit at the Cas9-induced double-stranded break, we designed an asymmetric ssDNA repair oligonucleotide having 34 bases upstream and 60 bases downstream of the beginning of the PAM site [24]. The oligo had a two-base pair (bp) substitution that changed the Asn at position 314 to Ile, a second silent substitution that created a TaqI restriction site, and a third silent substitution that disrupted the PAM site (Fig. 1C). The *dpy-10* co-conversion edit was accomplished with pDD162 derivative plasmids (pTS5 and pTS6) harboring the *dpy-10* guide. The ssDNA repair oligo to induce the *dpy-10(cn64)* dominant mutation was as described in ARRIBERE *et al.* [21]. The *spe-50*

and *dpy-10* CRISPR/Cas9 plasmids and repair oligos were injected into the gonads of N2 hermaphrodites.

A knockout mutation that affects both isoforms of *spe-47* was accomplished with the Alt-R™ CRISPR/Cas9 components (Integrated DNA Technologies™) for *in vitro* assembled Cas9-crRNA-tracrRNA ribonucleoproteins (RNPs) following the protocol of KOHLER *et al.* [25]. The *spe-47* target sequence was chosen using the CRISPR guide-finding feature in Geneious R11 (5'-AGTTGCCAGTGACTCCAACA-3'). A specific *spe-47* edit that affects both spliced isoforms was designed into an ssDNA repair oligo. The oligo consisted of 55 bp upstream and 58 bp downstream of the beginning of the PAM site. The oligo had an altered sequence that disrupted five of the six bp just upstream of the PAM site, induced an NheI site that created an in frame stop codon, and inserted one bp to shift the reading frame (Fig. 1).

To induce the *spe-47* knockout, we incubated equimolar solutions of our target-specific crRNAs (for both *spe-47* and *dpy-10*) and standard tracrRNA (100 µM each) in IDT Nuclease-Free Duplex Buffer at 95 °C for 5 minutes followed by 5 minutes at room temperature. The RNA duplex and Cas9-NLS were combined for a final concentration of 27 µM each and incubated at room temperature for 5 minutes to form the final ribonucleoprotein (RNP). We injected worm gonads with a mixture of 17.5 µM RNP and 6 µM ssDNA repair template for *spe-47* along with 0.5 µM ssDNA repair template for *dpy-10*.

To recover the *spe-50* edit, 38 F1 rolling *cn64/+* worms were recovered and isolated. After laying eggs, the F1 worms placed in tubes; their DNA was then extracted and used as template in 5 µl PCR reactions with primers that flank the edit site (Forward primer: 5'-CATCAAGGGTGGACTTCTCG-3'; Reverse primer: 5'-AGCAGCAATGAGATGAGTGTCC-3'). To

150 the completed PCR reactions, we added 5 µl containing restriction enzyme buffer and 5
151 units of TaqI. After an hour of incubation, the components were run on agarose gels to
152 determine if the edit was induced. Of the 38 F1 rollers isolated, four appeared to have the
153 edit via their restriction digested PCR products. Only one of them was pursued, and it
154 contained the correct alteration of base pairs (Fig 1).
155
156 **Fig 1. Comparison of *spe-47* and *spe-50* sequences.** (A) Exonic structure of *spe-47* and
157 its paralog *spe-50*. Shown are the locations of sequence variants for these genes. (B)
158 Alignment of the SPE-47 and SPE-50 protein sequences. Darker background indicates
159 greater similarity, and mutations are shown in red. Near the carboxy terminus a line with
160 open arrows indicates the partial MSP domain, where the open arrows correspond to the
161 seven β strands present in *A. suum* MSP-α. Note that the MSP domains are truncated at the
162 carboxy terminus, missing the segment indicated by the downward bend in the MSP
163 marker line. Also, the region encoded by the *spe-47* isoform B is indicated by the green line.
164 (C) Two mutations created in this study. The original gene sequence is shown above with
165 the edited mRNA sequence below. The *zq27* mutation created in *spe-47* creates a stop
166 codon (underlined in red) within an NheI restriction enzyme site for detection and a 1 bp
167 insertion to shift the reading frame. The *zq26* mutation in *spe-50* induced an Asn to Ile
168 mutation in the position corresponding the *hc198* mutation in *spe-47*. Sequencing traces
169 shown confirmation that the sequences were edited in the mutant strains.
170
171 For *spe-47*, after injecting the constituted CRISPR/Cas9 RNPs, we found no F1
172 rollers. We combined three non-rolling F1s per petri dish in eight dishes, and extracted

their combined DNA for PCR/restriction analysis as previously described. One plate appeared to harbor a mutant. After isolating 24 offspring from this plate, we recovered a single worm that was homozygous for the edit (Fig 1). These mutations were designated *spe-50(zq26)* and *spe-47(zq27).*

Construction of a *spe-50* translational reporter

We created an N-terminal mCherry translational reporter construct for *spe-50* following the MosSCI technique [26, 27]. The mCherry sequence, amplified without its stop codon from plasmid pCFJ104 (Addgene), was placed directly downstream of 1,714 bp of the *spe-50* promoter sequence and was followed by the *spe-50* genomic sequence and 448 bp of the 3' UTR. All worm sequences were amplified from N2 DNA, and all PCR was performed with Phusion High Fidelity DNA Polymerase (Thermo Scientific). The sequences were amplified with PCR primers engineered with regions of ~20 bp overlap, enabling us to join them together following the PCR fusion technique described by Hobert [28]. The final fusion was cloned into the multiple cloning site of the vector pCFJ352, which targets the *ttTi4348* Mos1 insertion on Chromosome I for homologous recombination.

Microscopy, in vitro sperm activation, and microinjection transformation

Imaging was accomplished on a Nikon C2 confocal microscope also outfitted for Nomarski DIC and widefield epifluorescence. Widefield images were captured on a Nikon DS-Qi1 12 bit monochrome camera. Images were acquired and analyzed with Nikon NIS-Elements imaging software. All worms were dissected in SM1 buffer[29], and nuclear material was labeled with 30 ng/µl Hoechst 33342 in SM1 for live cells and with 20 ng/µl DAPI in PBS for fixed and permeabilized cells. Sperm were activated *in vitro* by exposure to

SM1 containing 200 µg/ml Pronase. Imaging of reporter constructs was kept constant across experiments to reduce error (e.g. the laser power and gain were used for each fluorophore/fluorescent label). Compounds were microinjected of into the gonads of recipient young adult hermaphrodites using a Nikon Eclipse Ti inverted microscope outfitted for Nomarski DIC.

Phylogenetic analysis

In order to estimate the evolutionary relationships of the SPE-50 homologous proteins and detect gene duplication events, we conducted a phylogenetic analysis using 15 protein sequences from 7 species of *Caenorhabditis*, with the protein OVOC10046 of *Onchocerca volvulus* as the outgroup. The analysis was run in MrBayes 3.2.6 [30] with the GTR + I model and two runs of six chains for 10 million repetitions, with a sampling interval of 1,000 repetitions and burn-in of 25%.

Results

spe-50 is a sperm gene and overlaps in expression with *spe-47*

When we first discovered that *spe-47* harbored the *hc198* mutation that suppressed *spe-27(it132ts)* sterility by inducing premature spermatid activation [18], we became aware that there was a closely-related paralog present in the genome: Y48B6A.5 (Fig 1 A&B). The SPE-47 and SPE-50 proteins exhibit a high degree of sequence conservation, with both having an N-terminus of unknown function and a C-terminal MSP domain that lacks the final ß strand (Fig 1 B). To determine if Y48B6A.5 expression is upregulated in sperm, we performed differential RT-PCR. The Y48B6A.5 transcript is abundant in *fem-3(q23)* mutant hermaphrodites (Fig 2); these worms produce only spermatids but are

otherwise somatically hermaphrodites. Alternatively, the transcript is nearly absent in *fem-1(hc13ts)* hermaphrodites that produce only oocytes. This pattern is characteristic of sperm genes.

Fig 2. RT-PCR results for the *spe-50* transcript. Primers specific for the Y48B6A.5 transcript amplified a robust product in *fem-3(q23ts)* hermaphrodites that produce only sperm, but such a product was nearly absent amplifying from *fem-1(hc13ts)* hermaphrodites that produce only oocytes. The *spe-50* transcript was also present in the N2 strain but not in the *spe-50(ttTi4488)* mutant that has the Mos1 transposon insertion in Exon 3. Had the transcript with the Mos1 transposon been amplified, it would have been 1,829 bp in length, and the extension time was designed to allow a product that large to be amplified. The PCR reactions also had primers for *act-2,* the *C. elegans* β-actin gene. The *act-2* product demonstrates that there was equivalent mRNA present in the samples. MW is the molecular weight marker: Phage lambda DNA digested with PstI.

There are two sperm genes mapped to the region of Y48B6A.5: *spe-7* [31] and *spe-18* (Steven L'Hernault, personal communication). In order to test whether Y48B6A.5 is actually one of the two nearby genes, we conducted complementation tests using the strain ZQ117 with the *ttTi4488* Mos1 transposon insertion in Y48B6A.5. This insertion disrupts Y48B6A.5 and results in the absence of a transcript (Fig 2). Hermaphrodites homozygous for mutations in *spe-7(mn252)* and *spe-18(hc133)* are sterile due to primary spermatocytes that arrest in Meiosis I [31; Steven L'Hernault, personal communication]. Males from the *ttTi4488* bearing strain were crossed with sterile *unc-4 spe-7* mutant hermaphrodites or

with sterile *spe-18* mutant hermaphrodites. The F1 hermaphrodites were isolated at 25 °C and their progeny counted. The F1 hermaphrodites had wild-type fertility: for *spe-7*, F1 fertility = 198 progeny (n=10, SEM=14.4), and for *spe-18*, F1 fertility = 190 progeny (n=12, SEM=9.3). Thus, the *ttTi4488* strain complemented both *spe-7* and *spe-18* because it carried wild-type alleles of both. Y48B6A.5 is a new sperm gene and was given the designation *spe-50* (Steven L'Hernault, personal communication).

To examine SPE-50 protein localization, we created an N-terminal translational reporter with mCherry via the mosSCI protocol [26, 27]. The mosSCI process inserts the reporter into specific chromosomal locations, allowing us to combine the *spe-50::mCherry* reporter with a *spe-47::GFP* reporter we created earlier [18] in a double reporter strain. Imaging of male gonads showed that SPE-50::mCherry colocalizes almost completely with SPE-47::GFP (Fig 3A). Both appear as small puncta surrounding nuclei that are entering the pachytene stage. The puncta enlarge and expand to fill the cells as they mature into primary spermatocytes. Both also then disappear as the secondary spermatocytes form with the spermatids being completely devoid of the reporters. No such fluorescence was found in males lacking the reporters (Fig 3B).

Fig 3. Localization of SPE-50::mCherry and SPE-47::GFP translational reporters in male gonads. The fluorescent images are 3D reconstructions of a stack of images. (A) The double reporter strain constructs and imaging in blue (nuclei), green (*spe-47::GFP*), and red (*spe-50::mCherry*). A region of the gonad in the merge image shown by the box is enlarged to give better detail of the localization. In this enlargement, only the middle of the 3D reconstruction is shown to give better understanding of colocalization. (B) Imaging from

the unlabeled wild-type strain for comparison. In both the reporter images and the wild-type control, there are remnants of the intestine present. The intestine is highly autofluorescent in green and red.

The colocalization of the two reporters in space and time suggested that these proteins are involved in the same cellular processes. We tested this hypothesis by examining mutations in both genes. The *spe-47* gene was discovered in a suppressor screen of *spe-27(it132ts)*. The *spe-27* mutation causes hermaphrodite sterility because the self-spermatids are unresponsive to the signal to activate [32]. The *spe-47(hc198)* mutation recovered from the screen causes some spermatids to activate precociously without the need for an activation signal, overcoming the sterility of *spe-27(it132ts)* (Fig 4) [18]. If SPE-50 is functionally redundant to SPE-47, then a mutation similar to *hc198* in *spe-50* should also result in precocious spermatid activation. Fig 1B shows the location of the amino acid changed by *spe-47(hc198)*: an isoleucine to asparagine substitution in the a_2 ß-strand of the MSP domain. Using CRISPER/Cas9, we induced the same amino acid change in *spe-50* by creating the *zq26* mutation. In addition to altering the two base pairs that cause the amino acid change, we made two other silent substitutions: one that created a TaqI restriction site to allow detection of the alteration, and the other that altered the PAM site to eliminate further Cas9 activity (Fig 1C). Interestingly, the *spe-50(zq26)* mutation did not suppress *spe-27(it132ts)* sterility (Fig 4). In fact, there was no fertility deficit associated with the *spe-50(zq26)* mutation, while *spe-47(hc198)* causes a significant reduction in fertility due to problems with sperm function (Fig 4) [18]. When both *spe-47(hc198)* and *spe-50(zq26)* were combined in the same strain, the fertility was nearly

identical to that of *spe-47(hc198)* alone (Fig 4). Thus, in terms of function, the two genes are not identical.

Fig 4. Suppression of *spe-27(it132ts)* sterility. *spe-27(it132ts)* mutants are sterile at 25 °C, but they regain some fertility if they are also homozygous for the *spe-47(hc198)* mutation. On its own, the *hc198* mutation results in a loss of fertility compared to wild type (N2). Conversely, the *spe-50(zq26)* mutation, which encodes the equivalent amino acid change as *hc198,* is entirely fertile on its own and does not suppress *spe-27(it132ts)* sterility. A strain with both *hc198* and *zq26* has approximately the same fertility as *hc198* on its own. Thus, the *spe-50(zq26)* mutation has no apparent effect on fertility.

We also examined knockout alleles of the two genes (Fig 1). Even though the *spe-50(ttTi4488)* transposon insertion disrupts *spe-50*, it had essentially no effect on fertility (Fig 5). In our previous study of *spe-47,* we created a knockout allele, *spe-47(zq19)* (Fig 1A), which caused only a slight reduction in fertility [18]. In the interim, a second isoform of the *spe-47* transcript, which is unaffected by the *spe-47(zq19)* mutation, was identified. To ensure that we disabled both isoforms, we inserted a stop codon and frame-shift in the fifth exon common to both isoforms to create a new knockout allele: *spe-47(zq27)* (Fig 1A and 1C). This new mutation also had little effect on fertility (Fig 5). Combining both *spe-50(ttTi4488)* and *spe-47(zq27)* mutations in the same strain of worms had only a modest effect on fertility, reducing it to just over 100 self-progeny per worm (Fig 5). Thus, these genes are not essential to spermatogenesis, but they do seem to have an interaction that reduces fertility when both gene products are absent.

Fig. 5. Fertility associated with *spe-47* and *spe-50* knockout mutations and *him* mutant backgrounds. In the top set of bars, the two knockout mutations are compared to N2 both alone and combined in the same strain. In the middle set of bars, the various knockout and *spe-27* suppressor mutations are combined with *him-8(e1489).* Both *spe-47* mutations in a *spe-50* knockout and *him-8* knockout background resulted in a drastic reduction of fertility. This reduction was due to a defect in sperm, because mating the strain to *him-8* males restored full fertility. In the bottom set of bars, combining the knockout mutations with *him-5* did not have a drastic reduction in fertility.

In creating strains, we noticed that combining the *him-8(e1489)* mutation with the two knockout mutations had a more profound effect on fertility (Fig 5). Combining either knockout alone with *him-8(e1489)* did not reduce fertility more than what we found in the *him-8(e1489)* strain alone. It was only when both knockouts were present in the *him-8* background that fertility was reduced approximately 15 progeny per hermaphrodite (Fig 5). This fertility deficit was due to self-sperm dysfunction, as mating these hermaphrodites to *him-8(e1489)* males increased their fertility greatly (Fig 5). Interestingly, combining the *spe-27*-suppressor mutation *spe-47(hc198)* with *spe-50(ttTi4488)* in a *him-8(e1489)* background lead to a similar drop in fertility. The same was not true when we combined the *spe-47(zq27)* knockout mutation with the *spe-27*-suppressor-like mutation *spe-50(zq26)* in a *him-8(e1489)* strain: the fertility was much higher (Fig 5). There was no similar fertility deficit associated with *him-5.* The triple *spe-47(zq27); spe-50(ttTi4488); him-5(e1490)* mutant hermaphrodites laid in excess of 50 offspring (Fig 5), indicating that

the interaction with *him-8* is not due just to X Chromosome non-disjunction problems common to both *him-5* and *him-8* mutants.

If the two knockout mutations in a *him-8(e1489)* background (the triple mutant) have defective sperm, then we might expect to see some defects in the sperm themselves. Of 145 sperm dissected from seven triple mutant males, all appeared as normal spermatids (Table I). This is similar to 162 sperm we dissected from five *him-8(e1489)* virgin males: all were spermatids. Because *him-8* has a role in X-Chromosome pairing and synapsis [33], we also looked for gross abnormalities in sperm nuclei. The vast majority of sperm from triple mutants had normal nuclei, similar to what we found for sperm from *him-8(e1489)* single mutants (Table I). Alternatively, spermatids from triple mutants could have defective activation, so we exposed spermatids to the *in vitro* activator Pronase [5, 34]. Sperm from triple mutants kept at 25 °C activated at a slightly but significantly reduced rate (88.5%) compared with sperm from *him-8(e1489)* mutants (96.3%) (Table I), although this does not seem a large enough effect to explain the fertility deficit in this strain. Finally, we looked at the sperm remaining in hermaphrodites one day after being transferred as L4s from 20 °C to 25 °C. The triple mutants had fewer sperm remaining in each gonad arm (mean = 31.7, SEM = 5.9, n = 21 gonad arms) than did *him-8* mutants (mean = 73.5, SEM = 6.9, n = 14 gonad arms), a significant difference (t=4.88, P<0.001). Again, this does not explain the small number of fertilized eggs produced by the triple mutants, because the number of sperm cells remaining per gonad arm is greater than the number of progeny produced by the triple mutants. In most instances, the sperm in the triple mutants were in or very near the spermatheca, while in others some sperm were well away from the spermatheca, being scattered in the uterus, as if they were unable to remain localized in

355 their target organ. Thus, overall there were more sperm remaining within triple mutants
356 than the number of fertilized eggs they produce, suggesting that these sperm are unable to
357 fertilize oocytes.
358
359 **Table I: Sperm activation and nuclear anatomy.**

Male dissected in	**Sperm morphology**		**Nuclear anatomy**		
SM1 buffer	Spermatids	Spermatozoa	Normal	Tiny	Double
Triple mutant	145	0	141	2	2
him-8	162	0	159	1	2
SM1 + Pronase*					
Triple mutant	15	116			
him-8	6	154			

360 Sperm phenotypes were examined in the triple mutant, *spe-47(zq27); spe-50(ttTi4488);*
361 *him-8(e1489)* with *him-8(e1489)* as the control. In SM1 buffer alone, dissected virgin males
362 release only inactive spermatids. In 200 µg/ml Pronase in SM1, spermatids activate to
363 crawling spermatozoa. The gross anatomy of sperm nuclei was examined in the worms
364 dissected in SM1, which also contained nuclear label Hoechst 33342 at 20µg/ml. *A G-test
365 of independence was performed on the data from Pronase activation: *P=0.011; G=6.456.*
366
367 We examined the phylogeny of *spe-50* and *spe-47* by comparing their protein
368 products to those from closely related species. The evolutionary analysis in Fig 6 shows
369 that the SPE-50 protein is clearly more closely related to orthologous proteins in the genus
370 than to its paralog-encoded SPE-47. Indeed, the hypothetical duplication of the ancestral
371 coding sequence must have taken place prior to the radiation of the species examined.
372

373 **Fig 6. Evolutionary relationship of the SPE-50 homologous proteins.** The proteins
374 were identified from a BLASTP search of the NCBI non-redundant protein sequence
375 database. For each protein, the accession number is listed before the slash, and the
376 WormBase identifier after the slash. The duplication event that resulted in creation of the
377 two paralogs occurred prior to the radiation of the species included in the analysis. The
378 phylogeny of the species within *Caenorhabditis* follows STEVENS *et al.* [35].
379

380 ## Discussion
381

382 The paralogs *spe-47* and *spe-50* have a high degree of protein sequence
383 conservation, and they retain a very similar exonic structure (Fig 1). Further, the gene
384 products are expressed in a nearly identical fashion within the spermatogenic tissue. Such
385 similarity would suggest a similar function. However, the two genes are not functionally
386 redundant, as the *spe-50(zq26)* mutation did not phenocopy its homologous *spe-47(hc198)*
387 mutation in suppressing *spe-27(it132ts)* sterility. Also, a strain with knockout mutations in
388 both genes had only slightly reduced fertility. Hypothetically, genes have multiple selection
389 pressures acting on their function, and these pressures may act in opposition, constraining
390 sequence evolution [36]. After a gene duplication event, the paralogs are thought to
391 undergo functional divergence to satisfy different selective pressures with opposing effects
392 on sequence evolution. Thus, true functionally redundant paralogs are very rare [36]. The
393 duplication event that gave rise to *spe-47* and *spe-50* occurred early in the radiation of the
394 genus (Fig 6), so the two paralogs have had ample time to evolve in response to different
395 selection pressures.

However, the *spe-47*and *spe-50* genes do show a phenotype when the knockout mutations are combined in a triple mutant strain with *him-8(e1489).* Fertility in the triple mutant strain is dramatically reduced due to a sperm defect. HIM-8 is a C2H2 zinc-finger protein that binds to the pairing center of the X-chromosome and initiates the pairing and synapsis of the X chromosome homologs [37]; *him-8* mutants show high levels of X-chromosome nondisjunction leading to increased rates of male production. HIM-8 protein binds to specific short sequences concentrated in the pairing centers, but these binding sequences are present at other sites on the X-chromosome and on the autosomes [38]. Thus, it is not surprising that HIM-8 protein is also bound more diffusely at other sites on the X chromosome and the autosomes [39]. Further, mutations in *him-8* can suppress the defects associated with hypomorphic mutations in *egl-13, pop-1, sptf-3,* and *lin-39*, each encoding a transcription factor [40]. The *him-8* mutations suppress only those transcription factor mutations that affect the DNA binding domains, prompting the hypothesis that HIM-8 also has a chromatin remodeling function that affects gene expression [40].

If the interaction of *him-8* with *spe-47* and *spe-50* is due to the chromatin remodeling role for HIM-8 protein, then it might be that the *him-8* mutation is altering the expression of other genes, one or more of which has a more direct interaction with *spe-47* and *spe-50.* We could not identify a sperm defect for the *spe-47; spe-50; him-8* triple mutants other than there were more sperm in the reproductive tract than fertilized eggs produced, suggesting a defect in fusion with the oocytes. SPE-47 localizes to the fibrous body-membranous organelle complexes [FB-MOs; 18], and by its colocalization with SPE-47, so does SPE-50. These complexes are involved in many aspects of sperm development, from acting as

419 vehicles for MSP transport during the meiotic divisions to the remodeling of the spermatid
420 during its transformation to an active spermatozoon. Many gene products are involved in
421 FB-MOs: at least nine different genes have mutant phenotypes that affect FB-MO
422 morphogenesis or function [10]. Here, our results suggest that, in combination with
423 altered gene expression from a HIM-8 deficit, the FB-MO-associated SPE-47 and SPE-50
424 proteins are important to the ability of sperm to fuse with passing oocytes, even though the
425 two proteins disappear before the spermatids form.

426 **Acknowledgements**

427 We are grateful to Steven L'Hernault for suggesting the complementation tests in
428 identifying the *spe-50* gene and in providing the *spe-50* designation.

429

References

1. Ma X, Zhu Y, Li C, Xue P, Zhao Y, Chen S, et al. Characterisation of *Caenorhabditis elegans* sperm transcriptome and proteome. BMC Genomics. 2014;15:168.

2. Reinke V, Gil IS, Ward S, Kazmer K. Genome-wide germline-enriched and sex-biased expression profiles in *Caenorhabditis elegans*. Development. 2004;131(2):311-23.

3. Muhlrad PJ, Ward S. Spermiogenesis initiation in *Caenorhabditis elegans* Involves a casein kinase 1 encoded by the *spe-6* gene. Genetics. 2002;161(1):143-55.

4. Nelson GA, Ward S. Vesicle fusion, pseudopod extension and amoeboid motility are induced in nematode spermatids by the ionophore monensin. Cell. 1980;19(2):457-64.

5. Ward S, Hogan E, Nelson GA. The initiation of spermiogenesis in the nematode *Caenorhabditis elegans*. Dev Biol. 1983;98(1):70-9.

6. Bandyopadhyay J, Lee J, Lee J, Lee JI, Yu JR, Jee C, et al. Calcineurin, a calcium/calmodulin-dependent protein phosphatase, is involved in movement, fertility, egg laying, and growth in *Caenorhabditis elegans*. Mol Biol Cell. 2002;13(9):3281-93.

7. L'Hernault SW. Spermatogenesis. In: Riddle DL, Blumenthal T, Meyer BJ, Priess JR, editors. *C elegans* II. Cold Spring Harbor, NY USA: Cold Spring Harbor Laboratory Press; 1997. p. 271-94.

8. Washington NL, Ward S. FER-1 regulates Ca2+ -mediated membrane fusion during *C. elegans* spermatogenesis. J Cell Sci. 2006;119(Pt 12):2552-62.

9. Liu Z, Wang B, He R, Zhao Y, Miao L. Calcium signaling and the MAPK cascade are required for sperm activation in *Caenorhabditis elegans*. Biochimica et biophysica acta. 2014;1843(2):299-308.

453 10. L'Hernault SW. Spermatogenesis. WormBook. 2006:1-14. Epub 2007/12/01. doi:
454 10.1895/wormbook.1.85.1. PubMed PMID: 18050478; PubMed Central PMCID:
455 PMCPMC4781361.
456 11. Smith JR, Stanfield GM. TRY-5 is a sperm-activating protease in *Caenorhabditis elegans*
457 seminal fluid. PLoS Genet. 2011;7(11):e1002375.
458 12. Fenker KE, Hansen AA, Chong CA, Jud MC, Duffy BA, Norton JP, et al. SLC6 family
459 transporter SNF-10 is required for protease-mediated activation of sperm motility in *C. elegans*.
460 Dev Biol. 2014;393(1):171-82.
461 13. Ellis RE, Stanfield GM. The regulation of spermatogenesis and sperm function in
462 nematodes. Semin Cell Dev Biol. 2014;29:17-30. Epub 2014/04/11. doi:
463 10.1016/j.semcdb.2014.04.005. PubMed PMID: 24718317; PubMed Central PMCID:
464 PMCPMC4082717.
465 14. Krauchunas AR, Mendez E, Ni JZ, Druzhinina M, Mulia A, Parry J, et al. *spe-43* is
466 required for sperm activation in *C. elegans*. Dev Biol. 2018;436(2):75-83.
467 15. Muhlrad PJ, Clark JN, Nasri U, Sullivan NG, LaMunyon CW. SPE-8, a protein-tyrosine
468 kinase, localizes to the spermatid cell membrane through interaction with other members of the
469 SPE-8 group spermatid activation signaling pathway in *C. elegans*. BMC genetics. 2014;15:83.
470 16. Gosney R, Liau WS, LaMunyon CW. A novel function for the presenilin family member
471 *spe-4*: inhibition of spermatid activation in *Caenorhabditis elegans*. BMC Dev Biol. 2008;8:44.
472 17. Liau WS, Nasri U, Elmatari D, Rothman J, LaMunyon CW. Premature sperm activation
473 and defective spermatogenesis caused by loss of *spe-46* function in *Caenorhabditis elegans*.
474 PloS one. 2013;8(3).

475 18. LaMunyon CW, Nasri U, Sullivan NG, Shaw MA, Prajapati G, Christensen M, et al. A
476 new player in the spermiogenesis pathway of *Caenorhabditis elegans*. Genetics.
477 2015;201(3):1103-16. doi: 10.1534/genetics.115.181172.
478 19. Brenner S. The genetics of *Caenorhabditis elegans*. Genetics. 1974;77(1):71-94. Epub
479 1974/05/01. PubMed PMID: 4366476; PubMed Central PMCID: PMCPMC1213120.
480 20. Vallin E, Gallagher J, Granger L, Martin E, Belougne J, Maurizio J, et al. A genome-
481 wide collection of Mos1 transposon insertion mutants for the *C. elegans* research community.
482 PLOS ONE. 2012;7(2):e30482.
483 21. Arribere JA, Bell RT, Fu BXH, Artiles KL, Hartman PS, Fire AZ. Efficient marker-free
484 recovery of custom genetic modifications with CRISPR/Cas9 in *Caenorhabditis elegans*.
485 Genetics. 2014;198(3):837-46. doi: 10.1534/genetics.114.169730.
486 22. Dickinson DJ, Ward JD, Reiner DJ, Goldstein B. Engineering the *Caenorhabditis*
487 *elegans* genome using Cas9-triggered homologous recombination. Nature Methods.
488 2013;10(10):1028-34. Epub 09/01. doi: 10.1038/nmeth.2641. PubMed PMID: 23995389.
489 23. Hsu PD, Scott DA, Weinstein JA, Ran FA, Konermann S, Agarwala V, et al. DNA
490 targeting specificity of RNA-guided Cas9 nucleases. Nature Biotechnology. 2013;31:827-32.
491 24. Liang X, Potter J, Kumar S, Ravinder N, Chesnut JD. Enhanced CRISPR/Cas9-mediated
492 precise genome editing by improved design and delivery of gRNA, Cas9 nuclease, and donor
493 DNA. Journal of Biotechnology. 2017;241:136-46.
494 25. Kohler S, Wojcik M, Xu K, Dernburg AF. Superresolution microscopy reveals the three-
495 dimensional organization of meiotic chromosome axes in intact *Caenorhabditis elegans* tissue.
496 Proc Natl Acad Sci U S A. 2017;114(24):E4734-E43.

497 26. Frokjaer-Jensen C, Davis MW, Ailion M, Jorgensen EM. Improved Mos1-mediated
498 transgenesis in *C. elegans*. Nature Methods. 2012;9(2):117-8.
499 27. Frokjaer-Jensen C, Davis MW, Hopkins CE, Newman BJ, Thummel JM, Olesen SP, et
500 al. Single-copy insertion of transgenes in *Caenorhabditis elegans*. Nat Genet. 2008;40(11):1375-
501 83.
502 28. Hobert O. PCR fusion-based approach to create reporter gene constructs for expression
503 analysis in transgenic *C. elegans*. Biotechniques. 2002;32(4):728-30.
504 29. Machaca K, DeFelice LJ, L'Hernault SW. A novel chloride channel localizes to
505 *Caenorhabditis elegans* spermatids and chloride channel blockers induce spermatid
506 differentiation. Dev Biol. 1996;176(1):1-16.
507 30. Ronquist F, Huelsenbeck JP. MrBayes 3: Bayesian phylogenetic inference under mixed
508 models. Bioinformatics. 2003;19(12):1572-4.
509 31. Sigurdson DC, Spanier GJ, Herman RK. *Caenorhabditis elegans* deficiency mapping.
510 Genetics. 1984;108(2):331-435.
511 32. Minniti AN, Sadler C, Ward S. Genetic and molecular analysis of *spe-27*, a gene required
512 for spermiogenesis in *Caenorhabditis elegans* hermaphrodites. Genetics. 1996;143:213-23.
513 33. Phillips CM, Wong C, Bhalla N, Carlton PM, Weiser P, Meneely PM, et al. HIM-8 binds
514 to the X chromosome pairing center and mediates chromosome-specific meiotic synapsis. Cell.
515 2005;123(6):1051-63. Epub 2005/12/20. doi: 10.1016/j.cell.2005.09.035. PubMed PMID:
516 16360035; PubMed Central PMCID: PMCPMC4435792.
517 34. L'Hernault SW, Roberts TM. Cell biology of nematode sperm. In: Epstein HF, Shakes D,
518 editors. Caenorhabditis elegans Modern Biological Analysis of an Organism. 48. San Diego:
519 Academic Press, Inc.; 1995. p. 273-99.

520 35. Stevens L, Félix M-A, Beltran T, Braendle C, Caurcel C, Fausett S, et al. Comparative
521 genomics of 10 new *Caenorhabditis* species. Evolution Letters. 2019;3(2):217-36.
522 36. Soria PS, McGary KL, Rokas A. Functional divergence for every paralog. Mol Biol Evol.
523 2014;31(4):984-92.
524 37. Phillips CM, Wong C, Bhalla N, Carlton PM, Weiser P, Meneely PM, et al. HIM-8 binds
525 to the X chromosome pairing center and mediates chromosome-specific meiotic synapsis. Cell.
526 2005;123(6):1051-63.
527 38. Phillips CM, Meng X, Zhang L, Chretien JH, Urnov FD, Dernburg AF. Identification of
528 chromosome sequence motifs that mediate meiotic pairing and synapsis in *C. elegans*. Nat Cell
529 Biol. 2009;11(8):934-42.
530 39. Nabeshima K, Mlynarczyk-Evans S, Villeneuve AM. Chromosome painting reveals
531 asynaptic full alignment of homologs and HIM-8-dependent remodeling of X chromosome
532 territories during *Caenorhabditis elegans* meiosis. PLoS Genet. 2011;7(8):e1002231.
533 40. Sun H, Nelms BL, Sleiman SF, Chamberlin HM, Hanna-Rose W. Modulation of
534 *Caenorhabditis elegans* transcription factor activity by HIM-8 and the related Zinc-Finger ZIM
535 proteins. Genetics. 2007;177(2):1221-6.
536

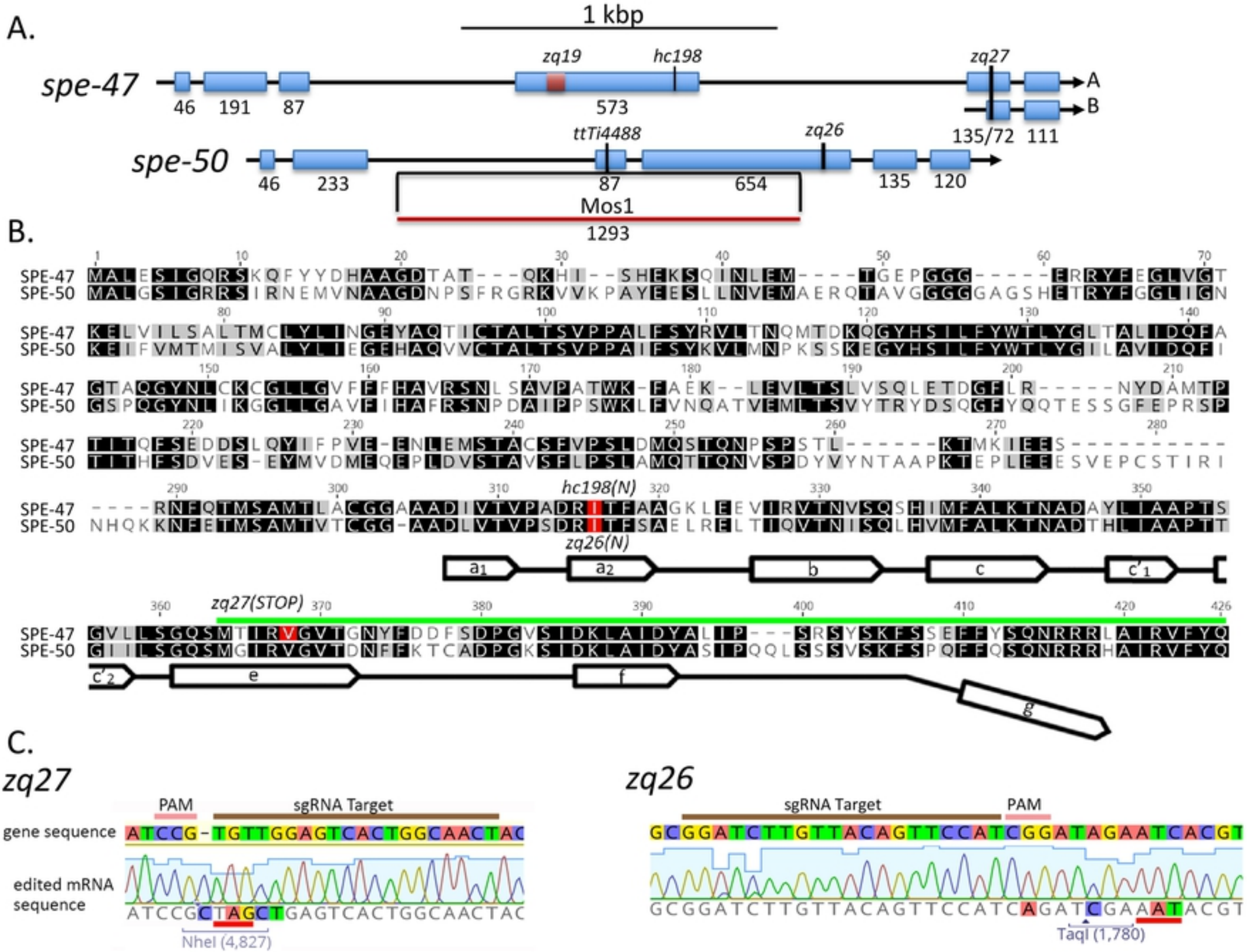
A.
1 kbp
spe-47
zq19
hc198
zq27
46
191
87
573
A
B
135/72
111
spe-50
ttTi4488
zq26
46
233
87
654
135
120
Mos1
1293
B.
SPE-47
SPE-50
hc198(N)
zq26(N)
a1
a2
b
c
c'1
zq27(STOP)
c'2
e
f
g
C.
zq27
PAM
sgRNA Target
gene sequence
ATCCG-TGTTGGAGTCACTGGCAACTAC
edited mRNA sequence
ATCCGCTAGCTGAGTCACTGGCAACTAC
NheI (4,827)
zq26
sgRNA Target
PAM
GCGGATCTTGTTACAGTTCCATCGGATAGAATCACGT
GCGGATCTTGTTACAGTTCCATCAGATCGAAATACGT
TaqI (1,780)

Figure 1

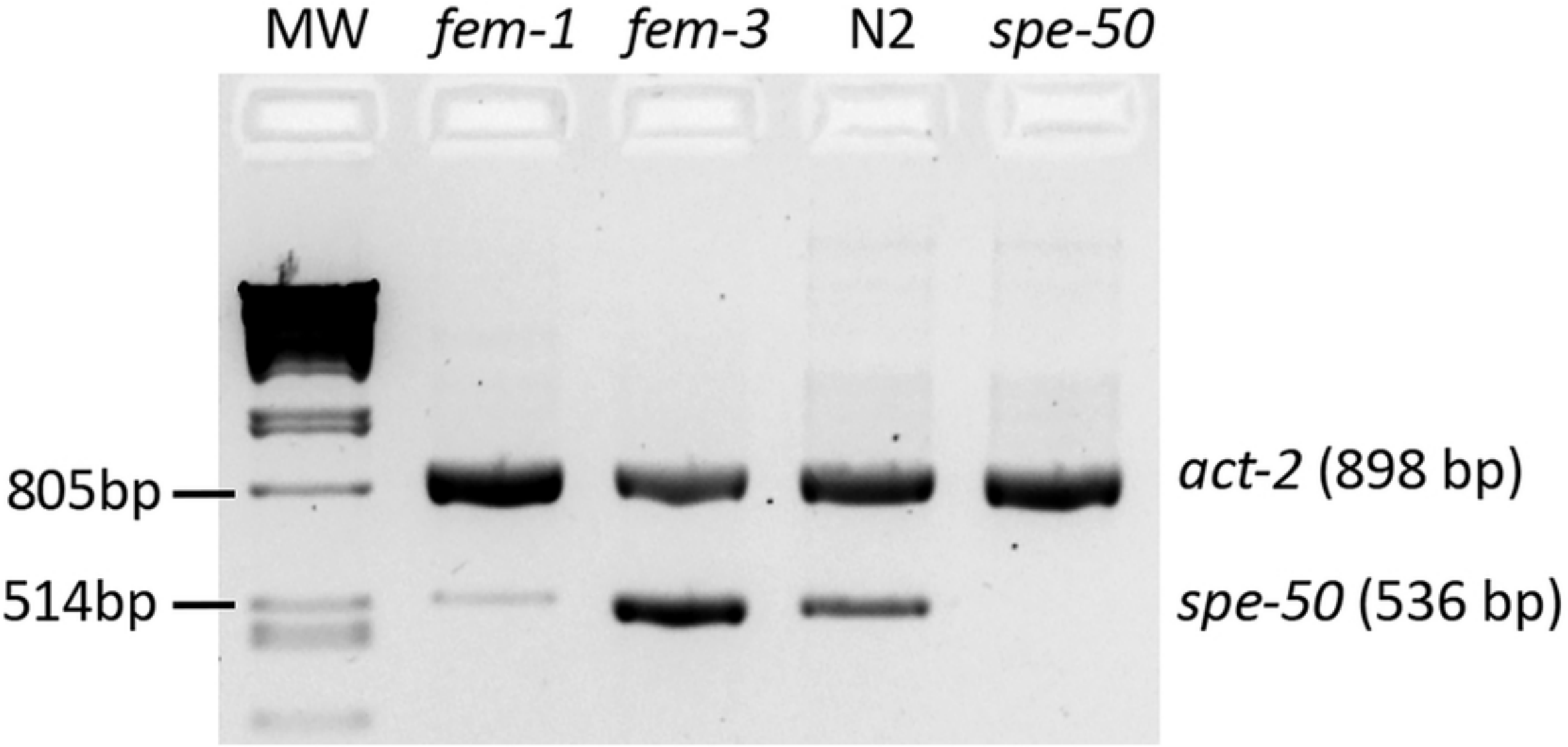

Figure 2

Figure 3

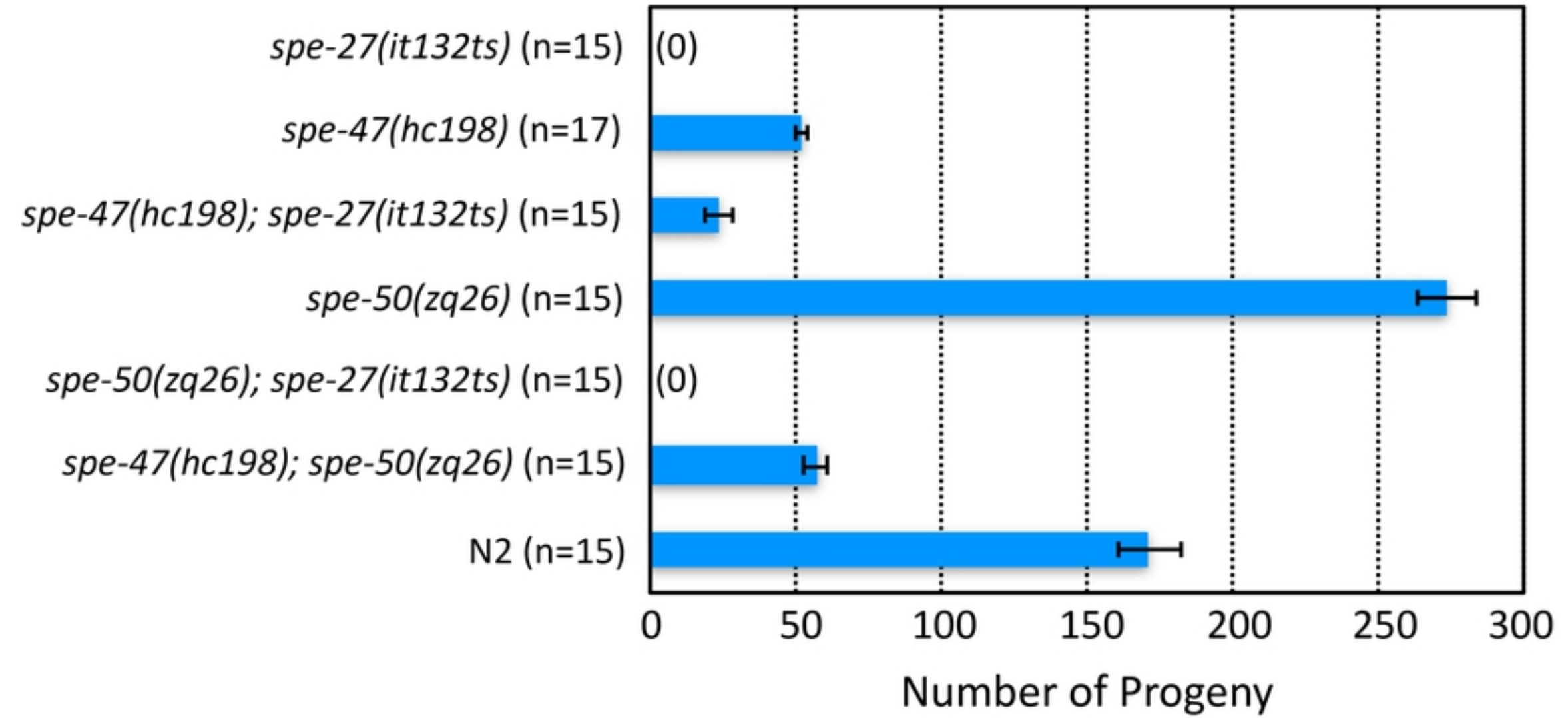
spe-27(it132ts) (n=15)
(0)
spe-47(hc198) (n=17)
spe-47(hc198); spe-27(it132ts) (n=15)
spe-50(zq26) (n=15)
spe-50(zq26); spe-27(it132ts) (n=15)
(0)
spe-47(hc198); spe-50(zq26) (n=15)
N2 (n=15)
0
50
100
150
200
250
300
Number of Progeny

Figure 4

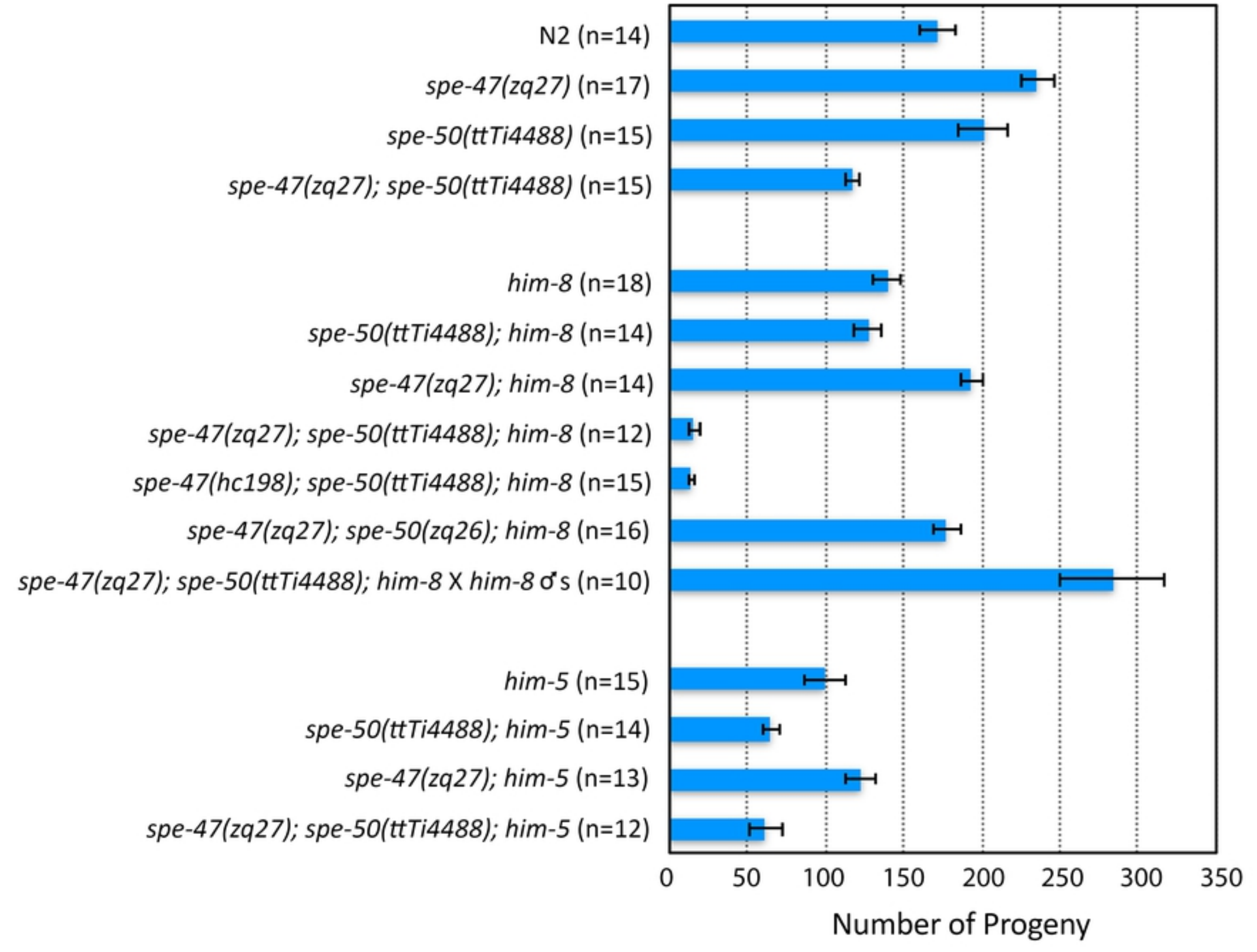
N2 (n=14)
spe-47(zq27) (n=17)
spe-50(ttTi4488) (n=15)
spe-47(zq27); spe-50(ttTi4488) (n=15)
him-8 (n=18)
spe-50(ttTi4488); him-8 (n=14)
spe-47(zq27); him-8 (n=14)
spe-47(zq27); spe-50(ttTi4488); him-8 (n=12)
spe-47(hc198); spe-50(ttTi4488); him-8 (n=15)
spe-47(zq27); spe-50(zq26); him-8 (n=16)
spe-47(zq27); spe-50(ttTi4488); him-8 X him-8 ♂s (n=10)
him-5 (n=15)
spe-50(ttTi4488); him-5 (n=14)
spe-47(zq27); him-5 (n=13)
spe-47(zq27); spe-50(ttTi4488); him-5 (n=12)
0
50
100
150
200
250
300
350
Number of Progeny

Figure 5

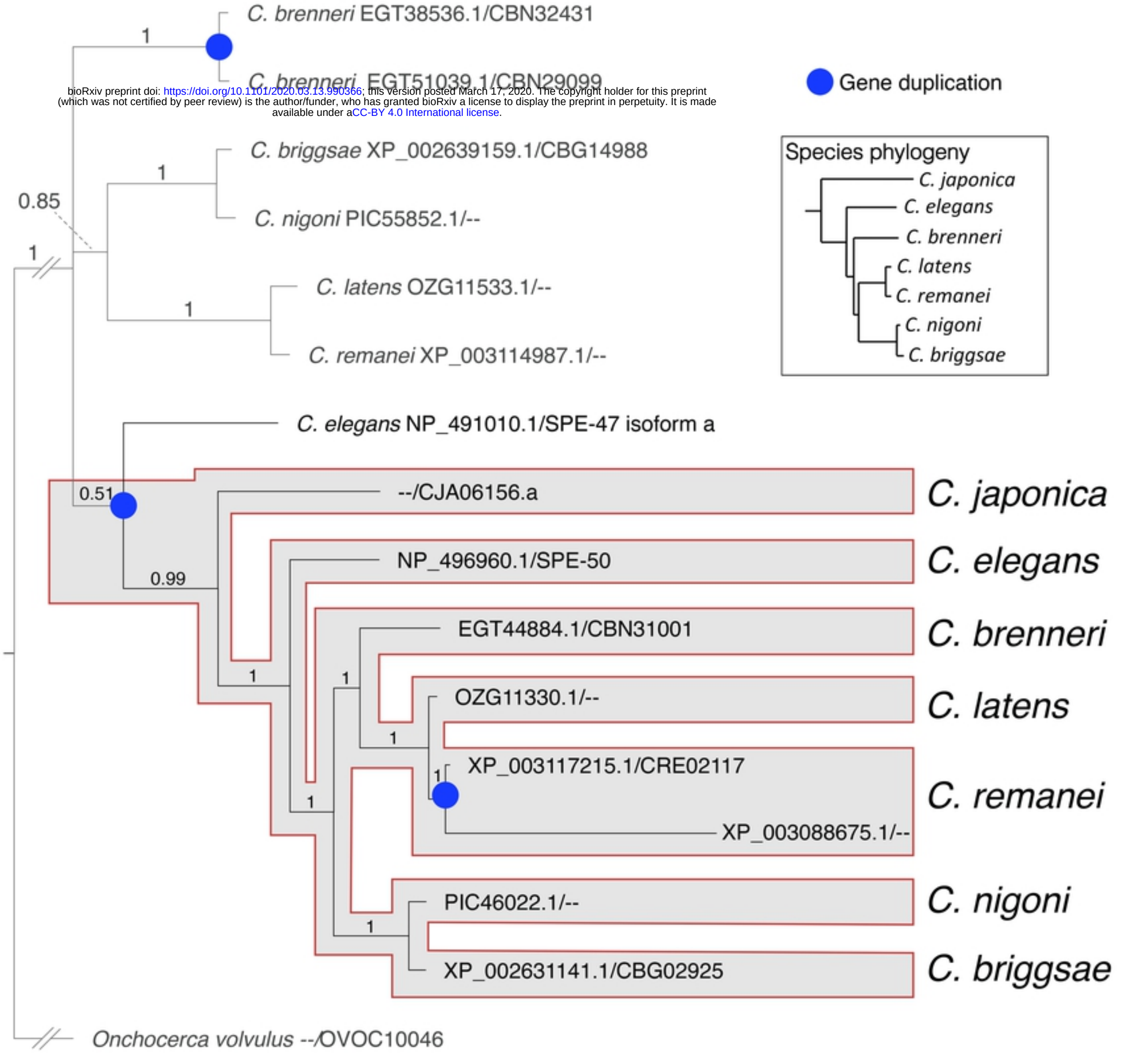

Figure 6